

СООБЩЕНИЯ
ОБЪЕДИНЕННОГО
ИНСТИТУТА
ЯДЕРНЫХ
ИССЛЕДОВАНИЙ
ДУБНА

E4-85-384

Dao Tien Khoa, K.V.Shitikova*

MICROSCOPIC DESCRIPTION
OF LIGHT-ION SCATTERING
FROM HEAVY SPHERICAL NUCLEI

* Moscow State University

1985

1. INTRODUCTION

In recent years, heavy-ion (HI) reactions induced by projectiles of mass number $A \leq 30$ have already been studied with good resolution^{/1/}. Even though the experimental data have been analysed rather successfully in the calculations of phenomenological models, a microscopic description of these processes is of a great interest for both experimental and theoretical investigations. Such a microscopic understanding of HI collisions may be founded on the calculation of the HI interaction potential using a realistic nucleon-nucleon (N-N) interaction^{/3/}. Note that for this purpose the folding model^{/4/} has proved to be a very convenient formalism, where the potential for HI scattering is obtained by averaging an appropriate N-N interaction over the nuclear densities of two colliding ions. In such an investigation the nuclear structure information is embodied in the nuclear wave functions that determine the ground-state and transition densities, and it is possible to calculate not only diagonal but also nondiagonal matrix elements of HI interaction, so, one can consider either elastic or inelastic scattering.

In the present work, within the folding model, elastic and inelastic scattering of ^3He , ^6Li and ^{16}O from heavy spherical nuclei has been studied with the ground-state and transition nuclear densities calculated by the method of hyperspherical functions^{/5/} and the quasiparticle-phonon nuclear model^{/2,9/} for projectiles and target-nuclei, respectively.

2. DETAILS OF CALCULATION

Usually, in the folding calculations there are always two basic ingredients. One is the construction of nuclear ground state and transition densities within the microscopic models, and the other is the choice of an appropriate effective N-N interaction between the projectile nucleons and the target nucleons. At first we give a brief description of the nuclear density calculation in the method of hyperspherical functions (MHF) and the quasiparticle-phonon nuclear model (QPM). Note that MHF and QPM have been applied to investigate HI scattering within the folding model in refs.^{/6-8/}. More details of this approach can be found in^{/8/} for example.

100 ... 1980 ...
1 510 ...
1980 ...

2.1. MHF and the Projectile Densities

In the K-harmonics method^{/5/} the total wave function of a nucleus with A nucleons is usually expanded in terms of K-harmonics polynomials $Y_{Ky}(\theta_i)$

$$\Psi(1,2,\dots,A) = \xi^{-\frac{1}{2}(3A-4)} \sum_{Ky} \chi_{Ky}(\xi) Y_{Ky}(\theta_i), \quad (1)$$

where $\gamma = [f] \epsilon LST$ ^{/5/}. With the wave functions calculated in the K-harmonics method^{/5/} one can obtain the ground-state and transition densities for a considered nucleus of A nucleons. In the present work we only consider the case of a single excitation of the nucleus-target, so the projectile is supposed to be in its ground state before and after the collision. Therefore, only the ground-state density of the nucleus-projectile of the form

$$\rho_0(r) = \frac{16\Gamma((5A-11)/2)}{\sqrt{\pi}\Gamma((5A-14)/2)} \int_0^\infty \frac{(\xi^2 - r^2)^{\frac{5A-16}{2}}}{\xi^{5A-13}} \chi_0^2(\xi) d\xi + \frac{8(A-4)\Gamma((5A-11)/2)}{3\sqrt{\pi}\Gamma((5A-16)/2)} \int_0^\infty \frac{r^2(\xi^2 - r^2)^{\frac{5A-15}{2}}}{\xi^{5A-13}} \chi_0^2(\xi) d\xi \quad (2)$$

is included into the folding calculations of this work.

2.2. QPM and the Target Densities

It is well known that in the inelastic HI scattering at bombarding energies ~10 MeV per nucleon, usually, the low-lying states of low multiplicities are excited (for example, 2^+ , 3^- , 4^+ , 5^- ... states of vibrational type in a spherical nucleus), so one needs to calculate within QPM, besides the ground-state density, the transition densities corresponding to such excitations in the nucleus-target. The general form of the QPM Hamiltonian is the following

$$H = H_{av} + H_{pair} + H_M + H_{SM}, \quad (3)$$

where H_{av} is the average field describing independent single-particle motions; H_{pair} describes the monopole pairing interaction between the neutrons or protons; H_M and H_{SM} are separable multipole and spin-multipole interaction terms generating the nuclear excitations. The explicit form of the QPM Hamiltonian is given in refs.^{/9/}, for example. In the single-particle basis calculation, the average field is taken as a Woods-Saxon potential. The potential parameter set used in the QPM and the

pairing constants are given in detail in ref.^{/10/}. After Bogolubov's transformation

$$a_{jm} = u_j \alpha_{jm} + (-)^{j-m} v_j \alpha_{j-m}^+, \quad (4)$$

where α_{jm}^+ and α_{jm} are the quasiparticle creation and annihilation operators, one can obtain the ground-state density for a heavy (spherical) nucleus in the form:

$$\rho_0(r) = \frac{1}{4\pi} \sum_j (2j+1) |R_j(r)|^2 v_j^2. \quad (5)$$

Here $R_j(r)$ is the radial part of the wave function for a single-particle state $j = (n, \ell, j)$. In further calculations the nuclear densities are normalized to

$$4\pi \int \rho_0(r) r^2 dr = A, \quad (6)$$

where A is the mass number of the nucleus. For the calculation of the wave functions of various excited states in the nucleus-target the QPM Hamiltonian is transformed into the phonon representation. In contrast with some other microscopic models where the phonons are introduced in a phenomenological way, within QPM the structure of phonons is calculated microscopically, in the random phase approximation (RPA), and the phonons are superpositions of various two-quasiparticle excitations

$$Q_{\lambda\mu}^+ \Psi_0 = \sum_{jj'} \psi_{jj'}^{\lambda\mu} [a_{jm}^+ a_{j'm'}^+]_{\lambda\mu} - (-)^{\lambda-\mu} \phi_{jj'}^{\lambda\mu} [a_{j'm} a_{jm}]_{\lambda-\mu} \Psi_0, \quad (7)$$

where Ψ_0 is the phonon vacuum. In the one-phonon approximation, i.e., in the RPA, the contribution from the term describing the quasiparticle-phonon interaction^{/9/} is absent, and one has for an excited state in the nucleus-target: $|\lambda_i^+\rangle = Q_{\lambda\mu}^+ \Psi_0$.

Further, if we define the nuclear transition density as

$$\rho(\vec{r}) = \langle f | \sum_k \delta(\vec{r} - \vec{r}_k) | i \rangle \quad (8)$$

with the multipole expansion of the form

$$\rho(\vec{r}) = \sum_{\lambda\mu} C_\lambda \langle J_i M_i \lambda \mu | J_f M_f \rangle \rho_\lambda(r) Y_{\lambda\mu}^*(\theta, \phi) \quad (9)$$

where the normalization constant C_λ is that defined in ref.^{/4/}, we get

$$\rho_\lambda(r) = \langle J_f M_f | \sum_k r_k^{-2} \delta(r - r_k) i^\lambda Y_\lambda(\theta_k, \phi_k) | J_i M_i \rangle. \quad (10)$$

In the case of single excitation of an even-even nucleus target ($J_f = \lambda$ and $J_i = 0$), after some transformations one obtains

$$\rho_\lambda(r) = \frac{1}{\sqrt{4\pi}} \sum_{j_1 \geq j_2} \frac{i^{\ell_2 + \lambda - \ell_1} j_2^{\lambda + \frac{3}{2}}}{2(1 + \delta_{j_1 j_2})} \hat{j}_1 \hat{j}_2 \begin{pmatrix} j_1 & j_2 & \lambda \\ \frac{1}{2} & -\frac{1}{2} & 0 \end{pmatrix} \quad (11)$$

$$\times R_{j_1}^*(r) R_{j_2}(r) u_{j_1 j_2}^{(+)} (\psi_{j_1 j_2}^{\lambda_1} + \phi_{j_1 j_2}^{\lambda_1}) [1 + (-)^{\ell_2 - \ell_1 + \lambda}].$$

2.3. HI Interaction Potential

There are various types of the effective N-N interaction which can be used in the folding calculations. In the present work we have chosen the so-called M3Y effective N-N interaction^{/11/} based upon a realistic G-matrix. The HI scattering is characterized by the strong absorption^{/3/}, i.e., the data is sensitive only to the tail of the HI potential in the vicinity of some strong absorption radius

$$R_{\text{crit.}} \approx 1.5(A_1^{1/3} + A_2^{1/3}) \quad (\text{fm}). \quad (12)$$

In such an approximation the double-folded potential may be written as

$$U_F(\vec{R}) = \int d\vec{r}_1 d\vec{r}_2 \rho_1(\vec{r}_1) \rho_2(\vec{r}_2) v(\vec{r}_{12} = \vec{R} + \vec{r}_2 - \vec{r}_1), \quad (13)$$

where ρ_1 and ρ_2 are the nucleon densities in the nuclei A_1 and A_2 respectively; $v(\vec{r}_{12})$, the effective N-N interaction between nucleons in A_1 and nucleons in A_2 . The calculation of six-dimensional integral (13) is very complicated in the coordinate space, but if we work in momentum space, this integral is reduced to a product of three one-dimensional integrals^{/3/}. With the multipole expansion (9) one obtains, in the case of single excitation of a spin-zero target, the following expression for double-folded potential (13)

$$U_F(\vec{R}) = C_\lambda U_\lambda(R) Y_{\lambda\mu}^*(\theta_R, \phi_R),$$

where

$$U_\lambda(R) = \frac{1}{2\pi^2} \int k^2 dk j_\lambda(kR) \vec{v}(k) \tilde{\rho}_\lambda^{(1)}(k) \tilde{\rho}_0^{(2)}(k) \quad (14)$$

and

$$\vec{f}_\lambda(k) = 4\pi \int r^2 dr j_\lambda(kr) \vec{f}_\lambda(r). \quad (15)$$

The M3Y interaction is

$$v(r) = 7999 \frac{\exp(-4r)}{4r} - 2134 \frac{\exp(-2.5r)}{2.5r} - 262 \delta(\vec{r}_{12}). \quad (16)$$

The inclusion of an explicit energy and density dependence into (16) generally leads to a better consistency of the calculational results with the experimental data (see ref.^{/12/}). The elastic scattering corresponds to $\lambda=0$ in these formulae. Further, $U_\lambda(R)$ is taken as a real part of the HI potential into the cross-section calculation. The imaginary part of the HI potential is included phenomenologically so as to fit the data for elastic cross-section. Usually^{/4/}, the imaginary optical potential is supposed to have a Woods-Saxon form

$$W(r) = - \frac{W_V}{1 + \exp[(r - R_V)/a]}, \quad (17)$$

where $R_V = r_V (A_1^{1/3} + A_2^{1/3})$; W_V , r_V and a_V are defined from the best fit to the elastic scattering data. In this case the imaginary transition potential is defined by deforming the Woods-Saxon potential (17), i.e.,

$$W_\lambda(r) = -\beta_\lambda^{(I)} R \frac{dW(r)}{dr}. \quad (18)$$

The deformation parameter $\beta_\lambda^{(I)}$ is obtained from the $B(E\lambda)$ values scaled according to $\beta R = \text{const}^{1/4}$. In some cases considered in this work, for the sake of simplicity, the imaginary part of the HI potential is supposed to have the same shape as the real part (in both elastic and inelastic channels). In such a simple approximation calculations have been performed with one adjustable parameter a equal to the ratio of the imaginary and real amplitudes of the HI optical potential.

3. RESULTS OF CALCULATION AND SOME DISCUSSIONS

The transition folded potential $U_\lambda(R)$ (14) must, generally, be used in the coupled channel calculations for the description of inelastic HI scattering. However, as it has been shown in other folding calculations^{/3,4/}, a qualitative agreement with the experimental data can be reached in the distorted-wave Born approximation (DWBA), especially, in the description of the lowest 2^+ , 3^- excited states in the nucleus-target, which have a strong one-phonon structure^{/1,2,9/}. In the present work all calculations have been performed within the DWBA using a modified version of the code DWUCK^{/13/}. The imaginary potential parameters have been defined from the best fit to the elastic data using an optical

model program with the search package MINUIT^{14/}. The phonon amplitudes ψ and ϕ have been calculated by the code RPAS^{16/} which performs the RPA calculations within QPM.

3.1. Scattering of $^3,^4\text{He}$

Although the true heavy ions have mass number $A > 4$, it is of interest to study $^3,^4\text{He}$ scattering by using microscopic nuclear densities for both the projectile and target. It should be noted that in recent years alpha scattering has been successfully investigated in the folding model with different types of effective forces, see, for example, ref.^{16/}. The possibility of the application of the M3Y interaction to the elastic alpha scattering has been discussed in ref.^{14/}. The inclusion of the energy and density dependence into M3Y interaction leads to a better consistency with the elastic and inelastic data^{17,18/} (In ref.^{18/} an experimental nucleon density was used for the alpha particle). Since in the first stage we are interested in a possible qualitative description of $^3,^4\text{He}$ scattering, the energy- and density-independent M3Y interaction (16) has been used in our folding calculations. The results of our calculation and experimental data^{20/} for inelastic cross-section of system $^3\text{He} + ^{208}\text{Pb}$ at 43.7 MeV are shown in fig.1. The structure of the first 2^+ , 3^- , 4^+ and 5^- excited states in has been calculated with the set of interaction constants which reproduces the excitation energies and transition probabilities shown in table 1. As one may see from fig.1, our calculation gives a good description for the inelastic data excepting the case of 4_1 excitation in ^{208}Pb when the calculated cross-section was multiplied by factor 0.67 to reproduce the data. On the whole, our results describe this reaction better than the folding calculation^{20/} with an effective interaction between the helium and target nucleon and the microscopic^{21/} transition densities for ^{208}Pb target. (The results of this calculation require strong renormalization factors for all the considered cases, for example, this factor is equal to 5.3 for the 4_1 case; and the calculated 5_1^- cross-section cannot fit the data at forward angles). Further, our calculation gives a rather good fit to the elastic and inelastic data^{22/} of alpha scattering on ^{208}Pb at 42 MeV (see fig.2) in such a simple approximation that the imaginary potential has the same shape as the real one (χ^2 is reduced by a factor of about two using a volume Woods-Saxon imaginary potential (17)). From the two cases considered above one may conclude that the $^3,^4\text{He}$ densities calculated in the MHF are quite adequate to be used in the description of elastic and inelastic $^3,^4\text{He}$ scattering within the folding model.

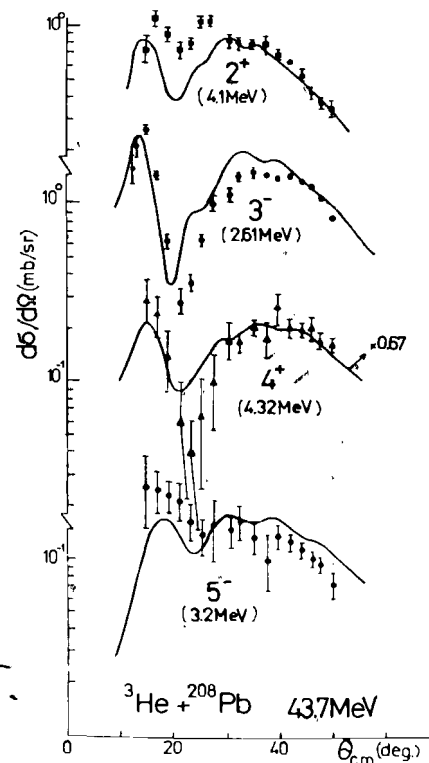


Fig.1. The calculated inelastic cross-sections for $^3\text{He} + ^{208}\text{Pb}$ at 43.7 MeV.

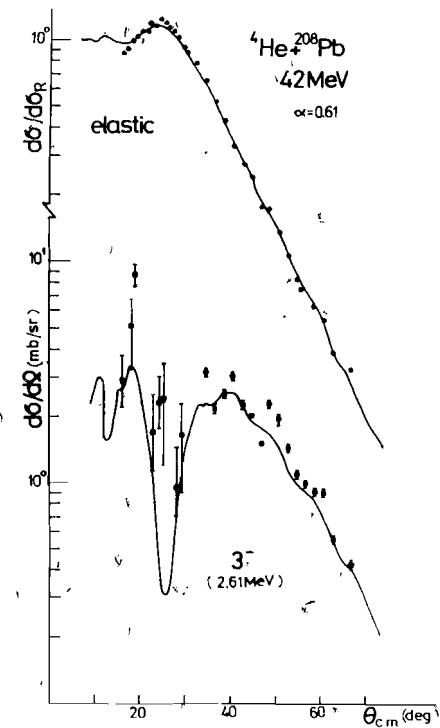


Fig.2. The calculated elastic and inelastic cross-sections for $^4\text{He} + ^{208}\text{Pb}$ at 42 MeV.

Table 1
The structure of the low-lying excited states in the nuclei-targets calculated in the RPA

Target	λ^π	ω_{λ^π} (MeV)		$B(E\lambda^\pi)$ (e^2b^2)		RMS(fm)
		expt.	calc.	expt.	calc.	
^{58}Ni	2^+	1.45	1.75	0.066, 0.099	0.083	3.823
^{60}Ni	2^+	1.33	1.87	0.092, 0.12	0.092	3.836
	3^-	4.04	4.27	0.016, 0.024	0.023	
^{90}Zr	2^+	2.19	2.63	0.06, 0.072	0.074	4.313
	3^-	2.75	2.72	0.074, 0.108	0.071	
^{208}Pb	2^+	4.086	4.64	0.30 ± 0.02	0.301	5.588
	3^-	2.61	2.64	0.69 ± 0.05	0.695	
	4^+	4.323	4.81	0.14 ± 0.01	0.141	
	5^-	3.194	3.2	0.046 ± 0.006	0.054	

3.2. Scattering of ${}^6\text{Li}$

The scattering of ${}^6\text{Li}$ is of a special interest because ${}^6\text{Li}$ appears to be "anomalous" within the framework of the folding model, where the folded potentials must be reduced in strength by a factor of about two^{4,23-25/} in order to fit the data. It also has been noted^{4/} that such an "anomaly" could not be due to an unwise choice of density distribution for ${}^6\text{Li}$ and it may be associated with the weak binding of that nucleus (in ref.^{25/} the folding analysis using an experimental^{26/} density distribution for ${}^6\text{Li}$ shows the same effect). In the MHF, calculation with the N-N potential B7^{27/} reproduces the mean squared radius $\text{RMS}=2.325$ fm. and minimum in the form factor of elastic electron scattering^{28/} $q = 5 \text{ fm}^{-1}$ compared to the experimental data ($\text{RMS}_{\text{expt.}} = 2.353$ fm and $q_{\text{expt.}} = 5 \text{ fm}^{-1}$) for ${}^6\text{Li}$ nucleus. The nucleon density of ${}^6\text{Li}$ calculated in this way within MHF has been used in the folding calculation^{27/} for elastic ${}^6\text{Li}$ scattering from different targets at not large bombarding energies, and a qualitative description of these processes has been obtained without renormalizing the strength of the folded potential. In the present paper we consider the elastic and inelastic scattering of ${}^6\text{Li}$ from ${}^{90}\text{Zr}$ and ${}^{58}\text{Ni}$ at energies 34 MeV and 71 MeV, respectively. The structure of excited states in ${}^{90}\text{Zr}$ and ${}^{58}\text{Ni}$ - targets shown in table 1 has been calculated within the RPA. Our calculation shows (see fig.3) that elastic and inelastic data for system ${}^6\text{Li}+{}^{90}\text{Zr}$ at 34 MeV^{29/} can be fitted rather well without introducing a renormalization coefficient N. However, the data for system ${}^6\text{Li}+{}^{58}\text{Ni}$ at 71 MeV^{30,31/} can be described only with introducing the coefficient N (see fig.4). The fit to the elastic data gives $\text{Re}N=0.53$ and $\text{Im}N=0.48$ in the case when the shape of the imaginary potential is the same as for the real one. If a volume Woods-Saxon imaginary potential (17) is used, χ^2 is reduced by several times, and a best fit to the elastic data is obtained with $N = 0.51$, $W_V = 17.57$ MeV, $r_V = 1.198$ fm, $a_V = 0.832$. Note, that these parameters are quite close to the ones obtained from folding analysis in ref.^{24/} Our calculations have shown that inelastic data can be reproduced only with introducing the same coefficient N for the transition folded potential as for the optical folded potential. This is consistent with the conclusion made by Satchler in ref.^{24/} The imaginary transition potential is obtained by deforming potential (17) with the value $\beta R = \text{const}$ for the lowest 2^+ state in ${}^{58}\text{Ni}$ taken from ref.^{30/} Thus, the renormalization of the folded potential by a coefficient of about 0.5 is also necessary in the calculation with ${}^6\text{Li}$ density from the MHF. (This is confirmed also in our calculations of ${}^6\text{Li}$ elastic scattering from different targets at 99 MeV^{23/}). We note that the conclusion made in ref.^{7/} from the descrip-

tion of ${}^6\text{Li}$ elastic scattering' cannot be taken as correct, and some attempts to explain microscopically such an anomalous behaviour of the nucleus ${}^6\text{Li}$ within MHF are now in progress.

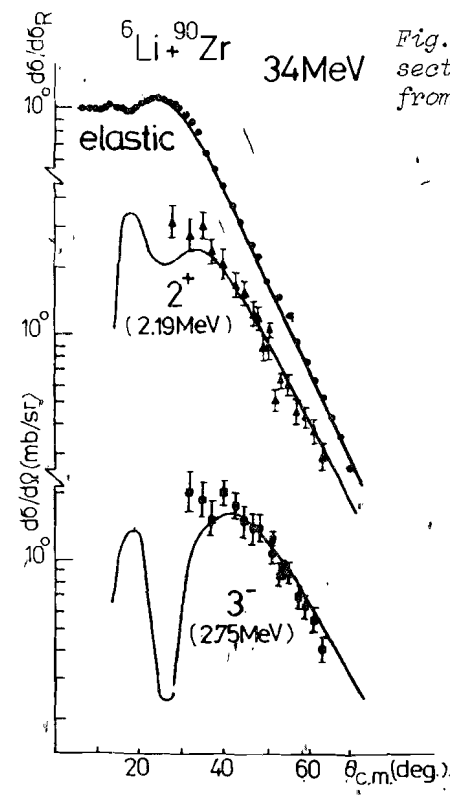


Fig.3. The calculated cross-sections of ${}^6\text{Li}$ scattering from ${}^{90}\text{Zr}$ at 34 MeV.

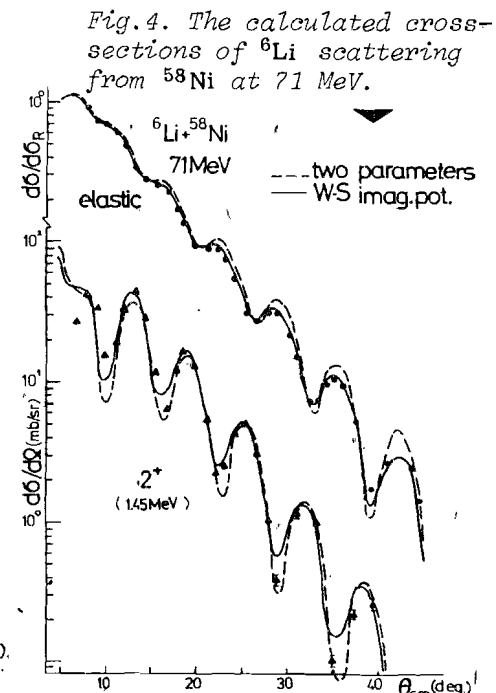


Fig.4. The calculated cross-sections of ${}^6\text{Li}$ scattering from ${}^{58}\text{Ni}$ at 71 MeV.

3.3. Scattering of ${}^{16}\text{O}$

The results of calculations and elastic and inelastic data for systems ${}^{16}\text{O}+{}^{60}\text{Ni}$ at energies 61.4 MeV^{33/} and 114 MeV^{34/}, ${}^{16}\text{O}+{}^{208}\text{Pb}$ at 104 MeV^{35/} are shown in figs.5-7. As one may see from these figures, our calculations give a good qualitative description for these reactions except for the case of 3_1^- excitation in ${}^{60}\text{Ni}$ induced by ion ${}^{16}\text{O}$ at 114 MeV (see fig.6). (In this case the calculated cross-section overestimates the data by a factor of about two and it is not understandable from the folding-model point of view). It is of interest for calculations with the nuclear densities from the MHF to study the influence of different types of the N-N potentials on the calculated cross-sections. An example of this is shown in fig.7, where the cross-sections are calculated with two different

Fig. 5. The calculated cross-sections of ^{16}O scattering from ^{60}Ni at 61.4 MeV.

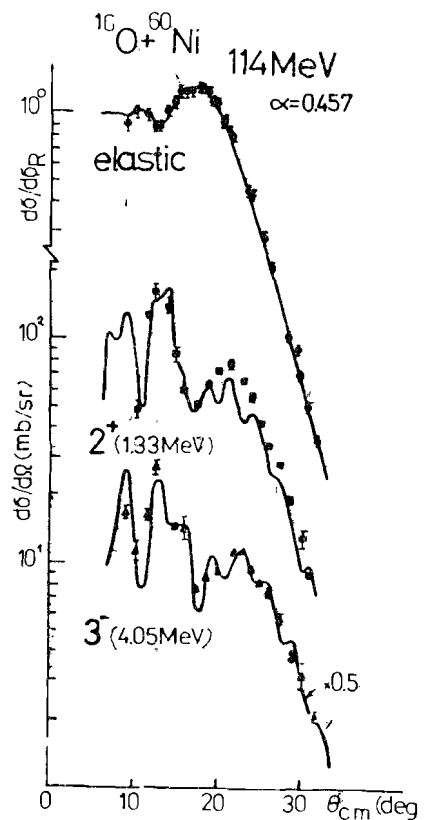
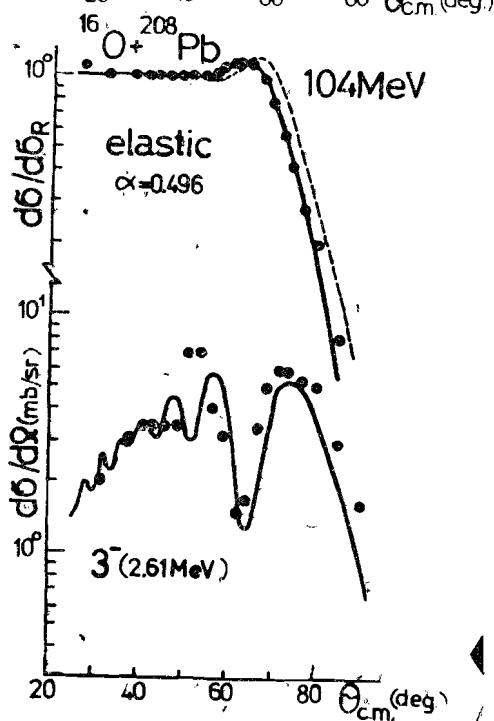
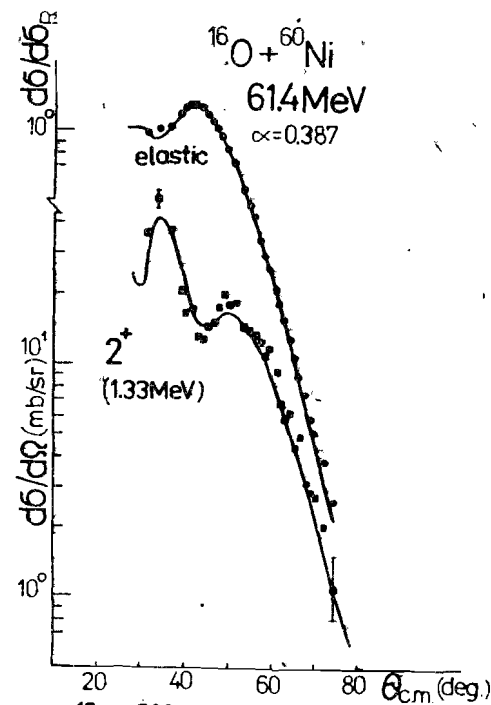


Fig. 6. The calculated cross-sections of ^{16}O scattering from ^{208}Pb at 104 MeV.

Fig. 7. The calculated cross-sections of ^{16}O scattering from ^{60}Ni at 114 MeV (see details in 3.3).

Table 2

The binding energy (E_b), excitation energy of the monopole resonance (E_{0+}), mean squared radius (RMS) and minimum in the elastic form factor of electron scattering (q) calculated in the MHF for some light nuclei-projectiles

Nucleus	E_b (MeV)		E_{0+} (MeV)		RMS (fm)		q (fm $^{-1}$)		Type of N-N potential used in MHF
	expt.	calc.	expt.	calc.	expt.	calc.	expt.	calc.	
^4He	28.3	29.3	20.2	26.4	1.482	1.728	5	5.4	B1/32/
^6Li	31.99	19.8		14.7	2.353	2.325	5	5	V7/27/
^{16}O	127.2	122.2		29.1	2.541	2.46	4	4.4	B4/32/
		106.3		22.9		2.66	4		B1

densities for ^{16}O . The ground-state density obtained with the N-N potential B1/32/ for ^{16}O gives a better fit to the data (the solid curves) than the density obtained with potential B4 (the dashed curve). (Some nuclear properties of ^{16}O calculated with these two types of the N-N potential are shown in table 2).

4. CONCLUSION

The microscopic nuclear models (the method of hyperspherical functions and quasiparticle-phonon nuclear model) are applied to study the elastic and inelastic heavy-ion scattering within the framework of the folding model. Results of our calculations reproduce the experimental data in most considered cases and this indicates the validity of further application of the MHF and QPM to the HI scattering.

The influence of the microscopic structure of the wave functions for considered nuclei on the calculated cross-sections is discussed.

The authors are indebted to Prof. V.G.Soloviev and F.A.Gareev for useful discussions.

REFERENCES

1. Broglia R.A., Winther A. Heavy Ion Reactions: Lecture Notes. Addison-Wesley, Reading, Massachusetts, 1981, vol.1.
2. Soloviev V.G. Theory of Complex Nuclei. Pergamon Press, Oxford, 1976; Soloviev V.G. Particles and Nuclei, 1978, vol.9, p.580.
3. Satchler G.R. Direct Nuclear Reactions. Oxford University Press, Oxford, 1983.
4. Satchler G.R., Love W.G. Phys.Rev., 1979, vol.55, p.183.

5. Shitikova K.V. Nucl.Phys., 1979, A331, p.365; Smirnov Yu.F., Shitikova K.V. Particles and Nuclei, 1977, vol.8, p.847;
6. Dymarz R., Shitikova K.V. JINR, E7-81-653, Dubna, 1981; Nazmitdinov R.G., Saupe G., Shitikova K.V. Yad.Fiz., 1984, vol.39, p.1415.
7. Dao Tien Khoa, Shitikova K.V. Yad.Fiz., 1985, vol.41, p.1166.
8. Dao Tien Khoa, Shitikova K.V. JINR, E4-85-143, Dubna, 1985.
9. Vdovin A.I., Soloviev V.G. Particles and Nuclei, 1983, vol.14, p.237; Voronov V.V., Soloviev V.G. ibid., 1983, vol.14, p.1381.
10. Ponomarev V.Yu. et al. Nucl.Phys., 1979, A323, p.446.
11. Bertsch G. et al. Nucl.Phys., 1977, A284, p.399.
12. Kobos A.M. et al. Nucl.Phys., 1982, A384, p.65.
13. Kunz P.D. University of Colorado, unpublished.
14. James F., Roos M. Comp.Phys.Comm., 1975, vol.10, p.393.
15. Stoyanov Ch., Yudin I.P. JINR, P4-11076, Dubna, 1977.
16. Gils H.J., Rebel H. Phys.Rev., 1976, C13, p.2159; Srivastava D.K., Rebel H. Kernforschungszentrum Karlsruhe, KfK 3735, Karlsruhe, 1984.
17. Kobos A.M. et al. Nucl.Phys., 1984, A425, p.205.
18. Pesl R. et al. Nucl.Phys., 1983, A313, p.111.
19. Sick I. Few Body System and Nucleon Forces II. (Ed. by H.Zingl et al.). Springer, Berlin, 1978, p.236.
20. Baker F.T., Tickle R. Phys.Rev., 1972, C5, p.544.
21. Gillet V., Green A.M., Sanderson E.A. Nucl.Phys., 1966, vol.88, p.321.
22. Alster J. Phys.Rev., 1966, vol.141, p.1138.
23. Schwandt P. et al. Phys.Rev., 1981, C24, p.1522.
24. Satchler G.R. Phys.Rev., 1980, C22, p.919.
25. Vineyard M.F. et al. Phys.Rev., 1984, C30, p.916.
26. Suelzle L.R., Yearian M.Y., Crannel H. Phys.Rev., 1967, vol.162, p.922.
27. Volkov A.B. Nucl.Phys., 1965, A74, p.33.
28. Burov V.V. et al. J.Phys.G: Nucl.Phys., 1981, vol.7, p.137.
29. Puigh R.J., Kemper K.W. Nucl.Phys., 1979, A313, p.363.
30. Williamson C. et al. Phys.Rev., 1980, C21, p.1344.
31. Huffman R. et al. Phys.Rev., 1980, C21, p.179.
32. Brink D.M., Boeker E. Nucl.Phys., 1967, A91, p.1.
33. Rehm K.E. et al. Phys.Rev., 1975, C12, p.1945.
34. Hansen O. et al. Nucl.Phys., 1983, A398, p.325.
35. Becchetti F.D. et al. Phys.Rev., 1972, C6, p.2215.

Received by Publishing Department
on May 23, 1985.

Лао Тиен Khoa, Шитикова К.В.
Микроскопическое описание рассеяния легких ионов
на тяжелых сферических ядрах

E4-85-384

Метод гиперсферических функций и квазичастично-фононная модель применяются для микроскопического изучения упругого и неупругого рассеяния тяжелых ионов. Потенциал взаимодействия тяжелых ионов рассчитывается в рамках фолдинг-модели с эффективным МЗУ нуклон-нуклонным взаимодействием. Изучаются рассеяния ^3He , ^6Li и ^{16}O на изотопах ^{58}Ni , ^{60}Ni , ^{90}Zr , ^{208}Pb . Поскольку информация о ядерной структуре содержится в ядерных волновых функциях, которые используются для вычисления ядерных плотностей сталкивающихся ядер, исследуется некоторое проявление микроскопической структуры волновых функций ядер в изучаемых реакциях. Результаты расчетов в целом хорошо воспроизводят экспериментальные данные, что указывает на надежность использования метода гиперсферических функций и квазичастично-фононной модели для микроскопического описания рассеяния тяжелых ионов.

Работа выполнена в Лаборатории теоретической физики ОИЯИ.

Сообщение Объединенного института ядерных исследований. Дубна 1985

Dao Tien Khoa, Shitikova K.V.
Microscopic Description of Light-Ion Scattering
from Heavy Spherical Nuclei

E4-85-384

The method of hyperspherical functions and the quasiparticle-phonon nuclear model are applied for microscopic study of elastic and inelastic heavy-ion scattering. The heavy-ion interaction potential is calculated within the folding-model using the M3Y effective nucleon-nucleon interaction. The scattering of ^3He , ^6Li and ^{16}O ions from $^{58,60}\text{Ni}$, ^{90}Zr and ^{208}Pb has been studied. Since the nuclear structure information is embodied in the nuclear wave functions that determine the nuclear densities of the colliding ions, some influence of the microscopic nuclear wave functions on the calculated cross sections has been investigated. Results of calculations reproduce the experimental data in most considered cases and this indicates the validity of further application of the method of hyperspherical functions and the quasiparticle-phonon model to the microscopic description of heavy-ion scattering.

The investigation has been performed at the Laboratory of Theoretical Physics, JINR.

Communication of the Joint Institute for Nuclear Research, Dubna 1985